





Cite this: *RSC Adv.*, 2018, 8, 20922

# Fluorescent supramolecular hydrogels self-assembled from tetraphenylethene (TPE)/single amino acid conjugates†

Nien-Tzu Chu, Rajan Deepan Chakravarthy,  Nai-Chia Shih, Yen-Hsu Lin, Yen-Chu Liu, Jhong-Hua Lin and Hsin-Chieh Lin \*

Herein, we report the synthesis of simple TPE/single amino acid conjugates, TPE-Ser and TPE-Asp with side-chains featuring functional groups that may provide an additional hydrogen bonding network for hydrogelation in aqueous medium. TPE-Ser, which has the lowest molecular weight, containing hydroxyl groups undergoes self-assembly into supramolecular hydrogels under physiological pH conditions. TPE-Asp with a carboxylic group side chain undergoes the self-assembly and hydrogelation processes under slightly acidic conditions (pH = 6.0). UV-vis, IR, PL and rheological studies clearly indicate the formation, stability and fluorescence properties of TPE-amino acid hydrogels. TEM micrographs of the hydrogels indicate that the compounds are self-assembled into a nanosheet morphology with random size and shape. Further, *in vitro* analysis of TPE-Ser and TPE-Asp with 3A6 cells shows that the compounds exhibit unique fluorescence signals in microcellular environments thus making them suitable candidates for bioimaging applications. Overall, these findings highlight the importance of the structure-hydrogelation relationship and provide new insights into the design of single amino-acid-based supramolecular hydrogels.

Received 15th March 2018  
Accepted 26th May 2018

DOI: 10.1039/c8ra02296h  
rsc.li/rsc-advances

## 1. Introduction

Supramolecular hydrogels with small peptide molecules have attracted much attention due to their significant biocompatibility and functionality.<sup>1–7</sup> Such molecules often require a  $\pi$ -conjugated hydrophobic group for the hydrogelation process. Many  $\pi$ -capped dipeptides or higher peptide amphiphiles are supramolecular hydrogelators because such molecules can participate in secondary structure formation predominantly as  $\beta$ -sheets through an interlocked molecular arrangement. The self-assembly of these secondary molecular structures together with the contributions of various weak non-covalent interactions such as hydrogen bonding, van der Waals forces, electrostatic forces and  $\pi$ - $\pi$  interactions result in 3D nanostructures that are capable of entrapping a large amount of water molecules to generate self-supporting hydrogels. Much of the literature pays particular attention to study the dipeptide or tripeptide based low molecular weight hydrogelators (LMWGs).<sup>6</sup> So far, however, there has been little discussion about single amino acid based hydrogelators.<sup>8–25</sup> For example, Xu and co-workers demonstrated the first explained the hydrogelation of *N*-(fluorenyl methoxycarbonyl) (Fmoc) protected single amino

acids through the molecular co-assembly process. Subsequently, the same group developed a novel enzyme triggered self-assembly/hydrogelation process for simple Fmoc-tyrosine phosphate compound.<sup>8</sup> Adams and co-workers studied the hydrogelation of commercially available Fmoc-amino acids using glucono- $\delta$ -lactone.<sup>13</sup> Nilsson and his group described the effects of side-chain halogenation, N-terminal groups and C-terminal modification on the self-assembly of Fmoc-phenyl alanine (Phe) derivatives.<sup>14–17</sup> Nandha *et al.* synthesized pyrene conjugated Phe hydrogels that capable of encapsulation vitamin B12 and doxorubicin.<sup>19</sup> Srivastava and co-workers developed alanine derivative based hydrogels that can encapsulate drug molecules such as doxorubicin.<sup>20,21</sup> Our research group has recently reported a number of naphthalimide and pyrene based single amino acid systems that form self-supporting hydrogels.<sup>22–25</sup> Although few supramolecular hydrogel materials prepared from simple amino acids are known in literature, there is still limited understanding about the structural and functional properties of such systems. This necessitates the development of more single amino-acid based supramolecular hydrogels.

Tetraphenylethylene (TPE) group possesses four aromatic rings, and is highly hydrophobic compared to the commonly used Fmoc system.<sup>8</sup> In addition, TPE derivatives have unique aggregation induced emission (AIE) property resulting from restriction of intramolecular ring rotation.<sup>26–31</sup> To date there is a substantial body of literature regarding the application of TPE-

Department of Materials Science and Engineering, National Chiao Tung University, Hsinchu, 300, Taiwan, Republic of China. E-mail: hclin45@nctu.edu.tw

† Electronic supplementary information (ESI) available: Synthesis and characterization. See DOI: 10.1039/c8ra02296h



based materials especially in the field of fluorescent chemosensors, bioprobes, optoelectronic materials, and supramolecular hydrogels.<sup>26–37</sup> Several TPE-containing supramolecular hydrogels have also been reported based on TPE/oligopeptide conjugates.<sup>35–37</sup> For example, TPE-Q19 (KRKR-SGSG-QQEFQFQFKQQ) formed a supramolecular hydrogel in the presence of NaCl. More recently, TPE-MAX (NH<sub>2</sub>-KRKRGSVKVKVKVDPPTVKVKVKV-Am) was demonstrated as a smart pH-switchable luminescent hydrogel. Previously, we conducted a systematic study of TPE-dipeptides and found that TPE-GG formed a supramolecular hydrogelator at pH 10.5.<sup>38</sup> For biological applications, there are still quite a lot of opportunities to improve for the amino-acid-based TPE compounds such as the hydrogelation ability under physiological pH. To achieve this, we can take advantage of the side chain of the functional amino acids with hydrogen-bond donor or acceptor.

In this work, we report on supramolecular hydrogelation and associated biological functions of simple TPE/amino acid conjugates. Serine (Ser) and aspartic acid (Asp) have been employed as amino side-chain because we hypothesized that such groups may exhibit additional hydrogen bonding network for hydrogelation in aqueous medium. Amino acids were combined with TPE group at the N-terminus through an amide linkage for the synthesis of amino acid derivatives. TPE-amino acid hydrogelators self-assembled in aqueous medium to generate pH sensitive hydrogels and detailed investigation suggests that the functional groups of amino acid side chain play a crucial role in self-assembly. Further, we investigated the *in vitro* analysis of TPE-Ser and TPE-Asp with immortalized human mesenchymal stem cells (3A6) and the results show that the compounds can exhibit blue fluorescent signals in microcellular environments thus making them as potential soft materials for bio-imaging applications.

## 2. Experimental

### 2.1 Synthesis

All starting materials and solvents were obtained from commercial sources and used as received. TPE-amino acid hydrogelators used in this study were prepared by solid phase peptide synthesis (SPPS) using classical Fmoc protocol. The purity of the final compounds was confirmed using <sup>1</sup>H-NMR, <sup>13</sup>C-NMR and MS studies. NMR spectra of the final TPE compounds were obtained on 300 MHz Varian Unity Inova NMR instrument in the deuterated solvents. High resolution mass spectra were obtained with Micromass Q-TOF MS spectrometer.

### 2.2 Gelation studies

Hydrogels were prepared by weighing 4 mg of sample (TPE-Ser or TPE-Asp) in a screw-capped 2 mL vial (diameter 10 mm). Aqueous NaOH solution was added and the resulting solution was vortexed for 5 s and sonicated for few minutes to dissolve the sample. Then the pH of the solution was carefully optimized using HCl to induce the self-assembly as well as hydrogelation (total volume: 200  $\mu$ L). Hydrogelation was

considered to have occurred when a solid-like material obtained did not exhibit any kind of gravitational flow (vial inversion test) during a period of 2–5 min in each case.

### 2.3 Transmission electron microscopy

The morphology of the TPE hydrogels was assessed using Hitachi HT7700 transmission electron microscope (TEM) operating at an accelerating voltage of 100 kV. The sample was prepared on carbon-coated copper grids by dropping a small amount of hydrogels (10  $\mu$ L) directly onto 200 mesh. Excess amount of the hydrogel was blotted using filter paper by capillary action, followed by negative staining the sample with uranyl acetate. The sample was then allowed to air-dry for 2 days before the images were captured.

### 2.4 Rheological tests

The visco-elasticity measurements of the hydrogels were carried out using TA discovery rheometer (DHR-1) using 40 mm parallel plate geometry. The pH adjusted TPE sample (400  $\mu$ L, 2 wt%) was sandwiched between stainless parallel plate geometry and a stationary bottom plate and the sample was allowed to stand for 2 hours before taking any rheological measurements. The storage modulus ( $G'$ ) and loss modulus ( $G''$ ) were measured at 25 °C as a function of frequency between the range of 0.1 rad s<sup>-1</sup> to 100 rad s<sup>-1</sup> at a constant strain of about 0.8%.

### 2.5 Spectroscopic studies

To understand various molecular interaction during hydrogelation the following spectroscopic studies were performed. UV-vis spectra were recorded with Jasco V-670 UV-visible spectrophotometer. CD experiments were carried out on a JASCO J-810 spectrometer. Fluorescence spectral studies were performed with Hitachi F-7000 fluorescence spectrophotometer. Fourier transform infrared spectroscopy (FTIR) measurements were carried out using a Perkin-Elmer spectrum 100 FT-IR spectrometer. For FTIR measurements, the TPE solution was cast on a ZnSe window. The sample was dried as thin film at room temperature under a constant stream of nitrogen. Each spectrum is an average of 20 scans at the resolution of 4 cm<sup>-1</sup>.

### 2.6 Cell viability tests

Biocompatibility assay of TPE-amino acid hydrogelators conjugates was evaluated through MTT cell viability test. Human mesenchymal stem cells (3A6, a gift from Dr Shih-Chieh Hung, China Medical University, Taiwan) and WS1 cells (CRL-1502, ATCC) were chosen as cell models for this study. The cells were pre-incubated into 24-well plates at a density of 5  $\times$  10<sup>4</sup> cells per well with 0.5 mL medium (DMEM for 3A6 cells and MEM-EBSS for WS1 cells) containing 10% FBS and 1% penicillin-streptomycin solution and incubated for 24 h. Then the culture medium was replaced with fresh medium. The stock solution of hydrogelators was prepared in DMSO at 10 mM concentration. Samples of different concentrations (10, 50, 100, 200, 500  $\mu$ M) prepared by diluting the stock solution with cell culture media, were then added and the cells were placed into



solution and incubated for 24 and 48 h, respectively. Then, the fresh medium supplemented with 0.5 mL of MTT reagent ( $4 \text{ mg mL}^{-1}$ ) was added per well and the cells were further incubated for another 4 h. The medium containing MTT was then removed and DMSO (0.5 mL per well) was added to dissolve the formazan crystals. The content of each 24-well was transferred to 96 well plate. The optical density of the resulting solution was measured at 595 nm, using an absorbance micro plate reader (Infinite F50, TECAN). Cells without TPE compounds were used as the control. The cell viability percentage was calculated by using the following formula: the cell viability percentage (%) =  $\text{OD}_{\text{sample}}/\text{OD}_{\text{control}}$ .

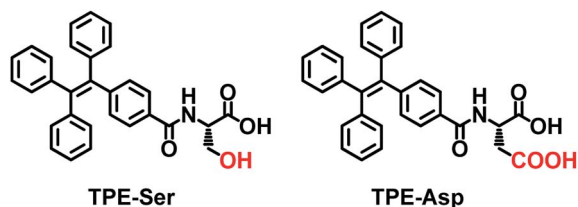
## 2.7 Cell-imaging studies

The cells were seeded on a 35 mm Petri dish at a density of  $5 \times 10^4$  cells per well and cultured for 24 h. TPE samples of various concentrations ( $10\text{--}50 \mu\text{M}$ ) were treated with 3A6 cells and incubated for 24 hours. After staining for suitable time, the cells were washed with phosphate-buffered saline for three times ( $\text{pH} = 7.4$ ) and images were acquired using laser-confocal microscope (Leica TCS-SP5-X AOBs).

# 3. Results and discussion

## 3.1 Synthesis and characterization of hydrogels

We began our study with the synthesis of 4-(1,2,2-triphenylvinyl) benzoic acid (TPE-acid) and the hydrogelators **TPE-Ser** and **TPE-Asp**. TPE-acid was synthesized following a general literature protocol.<sup>39</sup> The hydrogelators **TPE-Ser** and **TPE-Asp** were synthesized through the classical solid phase peptide synthesis (SPPS), which is an efficient way to produce peptide materials using 2-chlorotrityl chloride resin and Fmoc-protected amino acids. The resin was pre-swollen with dichloromethane and then a mixture of Fmoc-L-serine/Fmoc-L-aspartic acid and DIEA in dry DMF was added into the resin under anhydrous condition. Then the Fmoc-amino acid bounded resin was treated with piperidine to remove the Fmoc group. Finally, the coupling of N-capping agent TPE-acid was performed with amino acid-resin to obtain the desired products of **TPE-Ser** and **TPE-Asp** (See ESI† for details). The structure and purity of **TPE-Ser** and **TPE-Asp** were confirmed by standard spectroscopic methods, including proton nuclear magnetic resonance ( $^1\text{H-NMR}$ ), carbon nuclear magnetic resonance ( $^{13}\text{C-NMR}$ ) and electrospray ionization mass spectrometry (ESI-MS) analyses.



Scheme 1 The chemical structures of the **TPE-Ser** and **TPE-Asp** hydrogelators.

Scheme 1 shows the structures of the TPE capped amino acids investigated in this work. TPE was chosen as N-capping agent because it possesses significant hydrophobicity due to the presence of four phenyl rings. In addition, the TPE/peptide conjugates are AIE-active which is demonstrated in our previous reports.<sup>38</sup> Two non-aromatic functional amino acids such as serine and aspartic acid, were chosen for this study to generate extended hydrogen-bonded networks during self-assembly. TPE was covalently attached to the amino acids *via* a simple amide bond. After obtaining pure TPE-amino acid compounds, samples were tested for hydrogelation at various pH conditions (Table S1 and Fig. S1†). As shown in Fig. 1a and b, self-assembly of **TPE-Ser** molecules resulted in stable hydrogel at 2 wt% under a pH of 7.1. On the other hand, **TPE-Asp** required a slight acidic condition for hydrogelation ( $\text{pH} = 6.0$ , Fig. 1c and d). Both **TPE-Ser** and **TPE-Asp** compounds exhibited intensive fluorescence emission characteristics in their gel states (Fig. 1b and d).

To examine the macroscopic gel stability of the TPE hydrogels the inverted tube test and rheological measurements were carried out. Dynamic frequency sweeps were measured for **TPE-Ser** and **TPE-Asp** hydrogels and the results are shown in Fig. 1e and f. The storage modulus  $G'$  (elastic response) and loss modulus  $G''$  (viscous behaviour) are independent over the entire frequency range of 0.1–100 Hz (strain sweep results, see Fig. S2†). The average  $G'$  of **TPE-Ser** at 2 wt% was around 0.62 kPa. As stated before, **TPE-Asp** formed a stable gel only at acidic pH, and hence the hydrogels of both TPE compounds were prepared at  $\text{pH} = 6.0$  and rheological properties were compared (Fig. 1f and Table S1†). Notably, **TPE-Ser** ( $\text{pH} = 6.0$ ) gave the maximum  $G'$  value of around 1.1 kPa. The transition temperature ( $T_{\text{gel-sol}}$ ) of the hydrogels was measured and the results show that **TPE-Asp** is relatively stable gel, which is consistent with the rheological data (Table S1 and Fig. S3†).

Transmission electron microscopy (TEM) analysis of the hydrogel samples was carried out to understand the microstructures and morphologies of hydrogels and the images (Fig. 2) suggested that the hydrogels of both **TPE-Ser** and **TPE-**

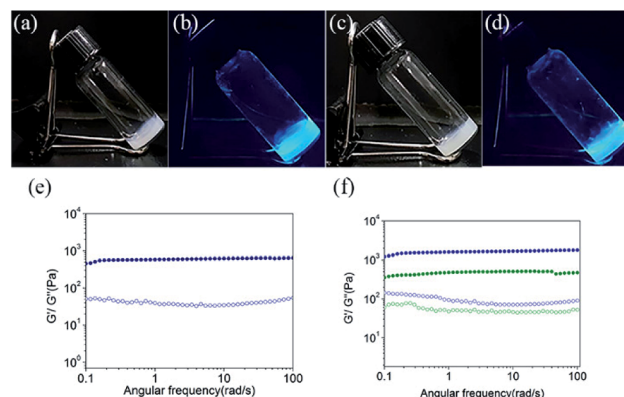


Fig. 1 Optical images of self-supporting hydrogels prepared from **TPE-Ser** (2% w/v,  $\text{pH} = 7.1$ , at (a) normal light, (b) UV light) and **TPE-Asp** (2% w/v,  $\text{pH} = 6.0$ , at (c) normal light, (d) UV light); frequency sweep rheological data for (e) hydrogel **TPE-Ser**,  $\text{pH} = 7.1$  and (f) hydrogels **TPE-Ser** (blue) and **TPE-Asp** (green),  $\text{pH} = 6.0$  (closed and open circles for  $G'$  and  $G''$ ).





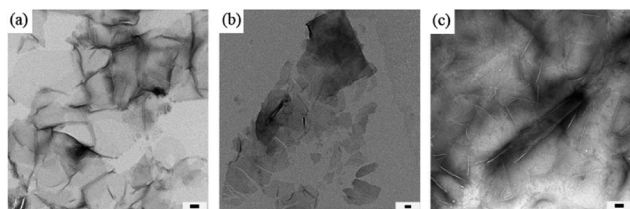


Fig. 2 TEM images of the hydrogels prepared from hydrogel (a) TPE-Ser, pH = 7.0, (b) TPE-Ser, pH = 6.0 and (c) TPE-Asp, pH = 6.0. The scale bar is 100 nm.

**Asp** samples consisted of nano-sheet like morphology with random size and shapes. Although supramolecular structures of the TPE molecules in the gel state can be visualized through TEM analysis, various other spectroscopic characterizations are indispensable requisite for understanding the molecular packing and photophysical properties. A number of spectroscopic techniques were used in this study, including UV-vis absorption, circular dichroism (CD) spectroscopy, Fourier transform infrared (FT-IR) spectroscopy and fluorescence emission (PL).

**TPE-Ser** and **TPE-Asp** revealed a strong absorption band at approximately 330 nm which is due  $\pi$ - $\pi^*$  electronic transition of aggregated TPE moiety (Fig. S4<sup>†</sup>).<sup>37,40,41</sup> CD spectra of **TPE-Ser** and **TPE-Asp** showed a bisignated Cotton effect signals within this region, indicating strong  $\pi$ -stacks of TPE chromophores in water (Fig. 3a and b). In addition, there is a strong CD signal was observed at 220 nm which might be attributed to the  $n$ - $\pi^*$  transition of symmetrically ordered L-amino acid residue.<sup>41</sup> To further explore the extend hydrogen bonding interactions in the assemblies, FT-IR spectra of **TPE-Ser** and **TPE-Asp** were studied in water and DMSO at gelation concentration (Fig. 3c and d). The FT-IR spectra of **TPE-Ser** and **TPE-Asp** at 2 wt% in aqueous solution show the amide I bands centered around  $1650\text{ cm}^{-1}$  in DMSO. When transitioning from DMSO to water, there is a significant shift in the bands to the lower energy region,

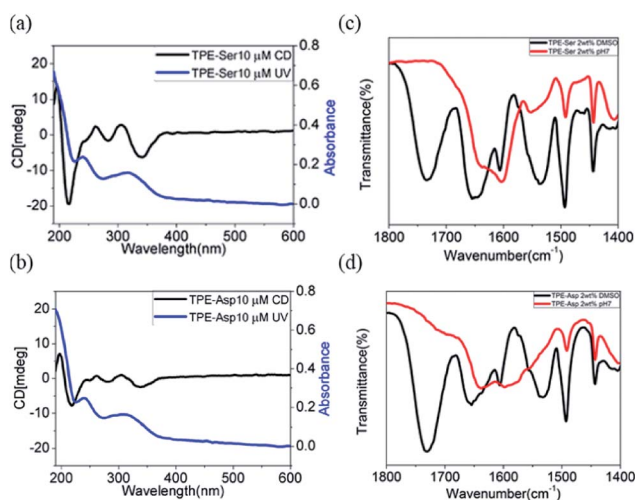


Fig. 3 CD (black line) and UV-spectra (blue line) of (a) TPE-Ser (10  $\mu\text{M}$ , pH = 7.0) and (b) TPE-Asp (10  $\mu\text{M}$ , pH = 6.0); FTIR spectra of (c) TPE-Ser and (d) TPE-Asp in water (red line) and in DMSO (black line).

suggesting the formation of extended hydrogen bonding network in the assemblies, which is consistent with CD observations. From these results, we conclude that the formation of self-assembled nano-sheets might be due extended hydrogen bonding interactions and strong stacking of TPE groups.

We further explored the fluorescence emission spectra of **TPE-Ser** and **TPE-Ser** in DMSO/water mixtures. For this study the **TPE-Ser** samples were prepared at 100  $\mu\text{M}$  in DMSO/water binary solvent mixtures with different water fractions (vol%) and Fig. 4a, shows their corresponding fluorescence intensity profile. **TPE-Ser** displayed a very weak emission in pure DMSO attributed to the monomeric form of TPE molecules. However, enhanced emission signals were observed when the water content ( $f_w$ ) is  $> 90\%$ . As the water fraction is increased to 99% and its PL intensities at 460 nm are 75-fold higher than that in pure DMSO solution (Fig. 4c). A similar effect was observed with **TPE-Asp** molecule with the PL intensity at 99% water content was  $\approx 60$ -fold higher than that in pure DMSO solution (Fig. 4b and d). TPE molecules in the monomeric form are non-emissive due to the intramolecular rotation of phenyl rings. However, upon aggregation such rotations of phenyl groups are restricted and hence the molecules exhibited enhanced fluorescence intensity. Concentration-dependent fluorescent responses have also been investigated to check the possible AIE behaviour of TPE molecules. The emission intensity signals of **TPE-Ser** and **TPE-Asp** compounds were increased with increase in the TPE concentrations. However, the signals were quenched at higher concentrations (Fig. S5<sup>†</sup>). Such emission pattern are very similar to that of the previously reported TPE gels.<sup>37</sup> Overall, the experimental data discussed above clearly validate the fluorescence property of the TPE-amino acid hydrogelators.

Since both the TPE based molecules possess significant photophysical behaviour, we then employed them for cell imaging application. For the cell imaging application it is first necessary to evaluate the potential biocompatibility of the

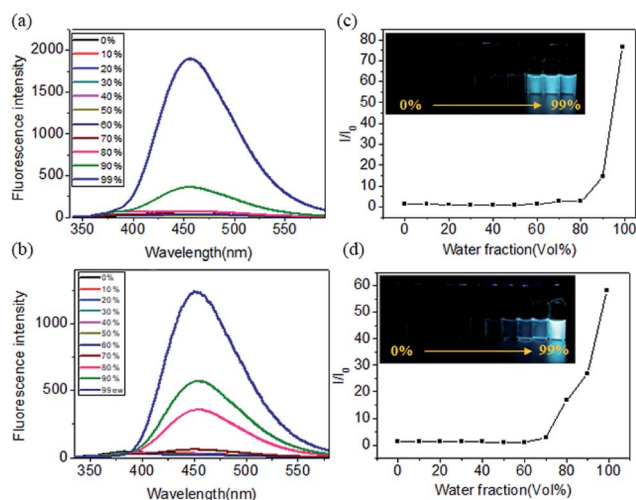


Fig. 4 PL spectra of (a) TPE-Ser (100  $\mu\text{M}$ , pH = 7.0) and (b) TPE-Asp (100  $\mu\text{M}$ , pH = 6.0) measured in DMSO/water mixture at various water fractions from 0 to 99%; (c) and (d) are the plots of florescent intensity ( $I/I_0$ ) versus the water fractions of TPE-Ser (at 320 nm) and TPE-Asp (at 315 nm), respectively.



material used. Biocompatibility studies of **TPE-Ser** and **TPE-Asp** were performed systematically by incubating them with 3A6 cell lines for 48 h by means of colorimetric MTT assay.<sup>42,43</sup> Fig. 5a and b shows the percentage viability of 3A6 cells treated with various concentrations of TPE-samples ranging from 10–50  $\mu\text{M}$ . Both **TPE-Ser** and **TPE-Asp** samples showed reasonable level of viability at 50  $\mu\text{M}$ . Similar conditions were used to study the biocompatibility with WS1 cells and the results are summarized in Fig. S6.† The half maximal inhibitory concentration ( $\text{IC}_{50}$ ) values being higher than 50  $\mu\text{M}$  for both the compounds indicated that the TPE compounds are biocompatible when concentration lowers than 50  $\mu\text{M}$  for 3A6 and WS1 cells (Fig. S6†). After studying the biocompatibility, we then evaluated the potential biomedical application of **TPE-Ser** and **TPE-Asp** for cell imaging application. 3A6 cells were treated with TPE compounds (10–50  $\mu\text{M}$ ) and observed under fluorescence microscope. After 24 hours of incubation the fluorescence microscopy images were taken (Fig. 5c–f, S7†). As shown in Fig. 5c–f, the hydrogelators **TPE-Ser** and **TPE-Asp** were aggregated in cytoplasm of the 3A6 cells thereby emitting strong blue fluorescence. Note that the average cell size for **TPE-Asp** imaging is somewhat smaller than that of **TPE-Ser** which may be attribute to the **TPE-Ser** has efficient self-assembly under pH 7.0. All of these data clearly showed that these hydrogelators may act as an efficient candidate for cell imaging applications.

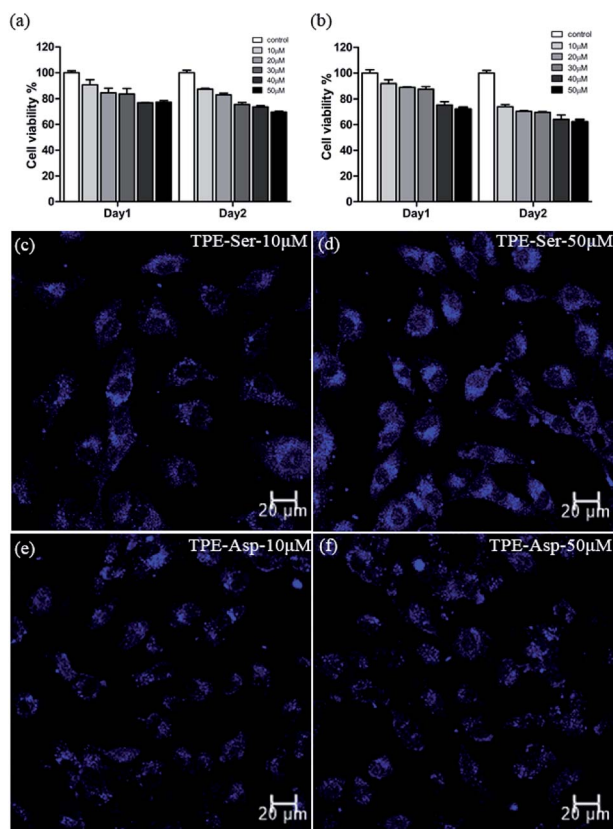


Fig. 5 Cell viability data of 3A6 cells incubated with 10–50  $\mu\text{M}$  of (a) **TPE-Ser** and (b) **TPE-Asp**; fluorescence microscopy images of 3A6 cells treated with different concentrations of **TPE-Ser** (c and d) and **TPE-Asp** (e and f), respectively. The scale bar is 20  $\mu\text{m}$ .

## 4. Conclusions

In summary, we have discovered low-molecular-weight hydrogelator made of simple amino acids (Ser and Asp) and TPE capping group. **TPE-Ser** has the lowest molecular weight and minimum number of atoms containing hydroxyl groups exhibited significant non-covalent interactions necessary for self-assembly/hydrogelations at physiological pH condition. In contrast, **TPE-Asp** needs mild acidic condition (pH = 6.0) for hydrogelation. Unlike TPE-dipeptides which form interlocked secondary structures, TPE-capped amino acids underwent self-assembly in aqueous medium *via* strong  $\pi$ -aggregates of TPE chromophores and extended hydrogen-bonding in aqueous condition into nanosheet structures as evidenced from various experimental techniques. From *in vitro* analysis of **TPE-Ser** and **TPE-Asp**, these compounds exhibit efficient fluorescent emission in microcellular environments thus making it suitable candidates for cell imaging applications.

## Conflicts of interest

There are no conflicts to declare.

## Acknowledgements

The study was supported by the Ministry of Science and Technology of the Republic of China, Taiwan (grant: MOST 106-2113-M-009-010).

## Notes and references

- X. Du, J. Zhou, J. Shi and B. Xu, *Chem. Rev.*, 2015, **115**, 13165.
- H. Wang, Z. Feng and B. Xu, *Chem. Soc. Rev.*, 2017, **46**, 2421.
- A. Dasgupta, J. H. Mondal and D. Das, *RSC Adv.*, 2013, **3**, 9117.
- X. Zhao and S. Zhang, *Chem. Soc. Rev.*, 2006, **35**, 1105.
- E. K. Johnson, D. J. Adams and P. J. Cameron, *J. Mater. Chem.*, 2011, **21**, 2024.
- E. R. Draper and D. J. Adams, *Chem*, 2017, **3**, 390.
- Z. Yang, G. Liang and B. Xu, *Acc. Chem. Res.*, 2008, **41**, 315.
- Z. Yang, H. Gu, Y. Zhang, L. Wang and B. Xu, *Chem. Commun.*, 2004, 208.
- Z. Yang and B. Xu, *Chem. Commun.*, 2004, 2424.
- Z. Yang, H. Gu, D. Fu, P. Gao, J. K. Lam and B. Xu, *Adv. Mater.*, 2004, **16**, 1440.
- J. Shi, Y. Gao, Z. Yang and B. Xu, *Beilstein J. Org. Chem.*, 2011, **7**, 167.
- J. Gao, H. Wang, L. Wang, J. Wang, D. Kong and Z. Yang, *J. Am. Chem. Soc.*, 2009, **131**, 11286.
- S. Sutton, N. L. Campbell, A. I. Cooper, M. Kirkland, W. J. Frith and D. J. Adams, *Langmuir*, 2009, **25**, 10285.
- D. M. Ryan, S. B. Anderson, F. T. Senguen, R. E. Youngman and B. L. Nilsson, *Soft Matter*, 2010, **6**, 475.
- D. M. Ryan, S. B. Anderson and B. L. Nilsson, *Soft Matter*, 2010, **6**, 3220.
- D. M. Ryan, T. M. Doran, S. B. Anderson and B. L. Nilsson, *Langmuir*, 2011, **27**, 4029.



- 17 D. M. Ryan, T. M. Doran and B. N. Nilsson, *Chem. Commun.*, 2011, **47**, 475.
- 18 S. Roy and A. Banerjee, *Soft Matter*, 2011, **7**, 5300.
- 19 J. Nanda, A. Biswas and A. Banerjee, *Soft Matter*, 2013, **9**, 4198.
- 20 A. M. Reddy and A. Srivastava, *Soft Matter*, 2014, **10**, 4863.
- 21 M. Singh, S. Kundu, M. A. Reddy, V. Sreekanth, R. K. Motiani, S. Sengupta, A. Srivastava and A. Bajaj, *Nanoscale*, 2014, **6**, 12849.
- 22 S.-M. Hsu, Y.-C. Lin, J.-W. Chang, Y.-H. Liu and H.-C. Lin, *Angew. Chem., Int. Ed.*, 2014, **53**, 1921.
- 23 L.-H. Hsu, S.-M. Hsu, F.-Y. Wu, Y.-H. Liu, S. R. Nelli, M.-Y. Yeh and H.-C. Lin, *RSC Adv.*, 2015, **5**, 20410.
- 24 S. R. Nelli, J.-H. Lin, T. N. A. Nguyen, D. T.-H. Tseng, S. K. Talloj and H.-C. Lin, *New J. Chem.*, 2017, **41**, 1229.
- 25 S. R. Nelli, R. D. Chakravarthy, Y.-M. Xing, J.-P. Weng and H.-C. Lin, *Soft Matter*, 2017, **13**, 8402.
- 26 K. R. Ghosh, S. K. Saha, J. P. Gao and Z. Y. Wang, *Chem. Commun.*, 2014, **50**, 716.
- 27 H.-T. Feng and Y.-S. Zheng, *Chem.–Eur. J.*, 2014, **20**, 195.
- 28 Y. Zhang, J. Xia, X. Feng, B. Tong, J. Shi, J. Zhi, Y. Dong and Y. Wei, *Sens. Actuators, B*, 2012, **161**, 587.
- 29 H. Liu, Z. Lv, K. Ding, X. Liu, L. Yuan, H. Chen and X. Li, *J. Mater. Chem. B*, 2013, **1**, 5550.
- 30 F. Hu, Y. Huang, G. Zhang, R. Zhao, H. Yang and D. Zhang, *Anal. Chem.*, 2014, **86**, 7987.
- 31 D. Ding, K. Li, B. Liu and B. Z. Tang, *Acc. Chem. Res.*, 2013, **46**, 2441.
- 32 Y. Liu, S. Chen, J. W. Y. Lam, P. Lu, R. T. K. Kwok, F. Mahtab, H. S. Kwok and B. Z. Tang, *Chem. Mater.*, 2011, **23**, 2536.
- 33 V. S. Vyas and R. Pathore, *Chem. Commun.*, 2010, **46**, 1065.
- 34 J. Huang, X. Yang, X. Li, P. Chen, R. Tang, F. Li, P. Lu, Y. Ma, L. Wang, J. Qin, Q. Li and Z. Li, *Chem. Commun.*, 2012, **48**, 9586.
- 35 C. Zhang, C. Liu, X. Xue, X. Zhang, S. Huo, Y. Jiang, W.-Q. Chen, G. Zou and X.-J. Liang, *ACS Appl. Mater. Interfaces*, 2014, **6**, 757.
- 36 C. Zhang, Y. Li, X. Xue, P. Chu, C. Liu, K. Yang, Y. Jiang, W.-Q. Chen and X.-J. Liang, *Chem. Commun.*, 2015, **51**, 4168.
- 37 A. M. Castilla, B. Dietrich and D. J. Adams, *Gels*, 2018, **4**, 17.
- 38 M.-Y. Yeh, C.-W. Huang, J.-W. Chang, Y.-T. Huang, J.-H. Lin, S.-M. Hsu, S.-C. Hung and H.-C. Lin, *Soft Matter*, 2016, **12**, 6347.
- 39 S. P. Bao, H. Ni, Q. H. Wu, H. Y. Gao, G. D. Liang, F. M. Zhu and Q. Wu, *Polymer*, 2014, **55**, 2205–2212.
- 40 R. Zhang, Y. Yuan, J. Liang, R. T. K. Kwok, Q. Zhu, G. Feng, J. Geng, B. Z. Tang and B. Liu, *ACS Appl. Mater. Interfaces*, 2014, **6**, 14302.
- 41 N. Amdursky and M. M. Stevens, *ChemPhysChem*, 2015, **16**, 2768.
- 42 K. Reichenbacher, H. I. Suss and J. Hulliger, *Chem. Soc. Rev.*, 2005, **34**, 22.
- 43 J. L. Guan, Cell Migration: Developmental Methods and Protocols, in *Methods in Molecular Biology*, Humana Press, vol. 294, 2005.

